

## PARAMETRIC STUDY OF NATURAL CONVECTIVE AND RADIATIVE HEAT TRANSFER IN INCLINED CYLINDRICAL ANNULI

Ass. Prof. Manal Hadi Al-Hafidh, \* Lina S. Safwat  
Mech. Engr. Dept., College of Engineering, University of Baghdad  
\*Mechanical Engineer, Ishtar\_121@yahoo.com

### ABSTRACT

The unsteady state laminar mixed convection and radiation through inclined cylindrical annulus is investigated numerically. The two heat transfer mechanisms of convection and radiation are treated independently and simultaneously. The outer cylinder was kept at a constant temperature while the inner cylinder was heated with constant heat flux. The study involved numerical solution of the governing equations which are continuity, momentum and energy equations using finite difference method (FDM), where the body fitted coordinate system (BFC) was used to generate the grid mesh for computational plane. A computer program (Fortran 90) was built to calculate the bulk Nusselt number ( $Nu_b$ ) after reaching steady state condition for fluid Prandtl number fixed at ( $Pr = 0.7$ ) (for air) with radius ratio ( $\hat{R} = 1.5, 2.6, 5.0$ ), Rayleigh number ( $0 \leq Ra \leq 10^3$ ), Reynolds number ( $50 \leq Re \leq 2000$ ), dimensionless heat generation ( $0 \leq Q \leq 10$ ), Conduction-Radiation parameter ( $0 \leq N \leq 10$ ), optical thickness ( $0 \leq \hat{t} \leq 10$ ) and different annulus inclination with horizontal plane ( $0^\circ \leq \delta \leq 90^\circ$ ). For the range of parameters considered, results show that radiation enhance heat transfer. It is also indicated in the results that  $Nu$  increase with the increasing of inclination angle  $\delta$ ,  $Ra$ ,  $Re$ ,  $\hat{R}$  and  $Q$ . The correlation equations are concluded to describe the radiation effect. Comparison of the result with the previous work shows a good agreement.

Keywords: Laminar, Mixed Convection, Radiation, Inclined Annulus.

### INTRODUCTION

Mixed convection has received a considerable attention from the thermo fluid point of view as well as the practical

interest of its engineering applications, since the associated fluid motion is largely interacted with the energy equation. Much theoretical and experimental work has

been published on this subject. Mixed convection in concentric annuli has been extensively studied for the past half century due to its wide applications in various engineering devices.

**Cheng and Hong [1]**, presented a numerical solution for the hydro dynamically and thermally fully developed combined free and forced laminar convection with upward flow in inclined tubes subjected to the thermal boundary conditions of axially uniform wall heat flux and peripherally uniform wall temperature at any axial positions. The results show that there was a limitation for Rayleigh number at which the back flow occurred. The tube inclination angle or body forced orientation effect on flow and heat transfer and show that in high Ra regime the tube orientation effect had a considerable influence on the results in the neighborhood of horizontal direction.

**Bohne and Obermeier [2]** studied mixed convection of upward and downward fluid flow in an internally heated concentric annulus in a vertical, inclined and horizontal position with annulus radius ratio of 0.742 and the heated core length to the equivalent diameter was 187.5. Water and water-glycol mixture were used as working medium. Experimental parameters covered were ( $350 \leq Re \leq 20000$ ,  $10^5 \leq Gr \leq 10^8$  and  $2.3 \leq Pr \leq 75$ ). The results show an increase of Nusselt number in the laminar flow range as the annulus inclination deviates from vertical to horizontal position. The measured heat transfer data were also presented in a form of correlation equations.

Theoretical and experimental study has been conducted by **Akeel Al-Sudani [3]** on mixed convection heat transfer of the flow through an inclined annulus with uniformly heated inner cylinder and adiabatic outer

cylinder with both fixed and rotating inner cylinder. Experiments were carried out to study the local and average heat transfer by mixed convection to a simultaneously developing air flow in a horizontal, inclined, and vertical concentric cylindrical annulus. The experimental setup consisted of an annulus which had a radius ratio of 0.555 and inner cylinder with a heated length 1.2m subjected to the constant heat flux while the outer cylinder was subjected to the ambient temperature.

Theoretical study were obtained and represented by stream function contours and isotherms as well as the axial velocity profile and circumferential distribution of local Nusselt number around the inner cylinder and the change of average Nusselt number with Rayleigh number.

The experimental results demonstrated the temperature variation along the inner cylinder surface and the local Nusselt number  $Nu_z$  variation with the dimensionless axial distance, for all angles of inclinations which show an increase in the  $Nu_z$  values as the heat flux increase and as the angle of the inclination moved from the vertical to the horizontal position.

Thermal radiation with simultaneous buoyancy and forced convection is an important issue for applications such as heat exchangers and cooling processes in nuclear reactors. In such systems, heat transfer results from coupled processes, in general, can not be calculated separately.

**Adegun and Bello-Ochende [4]** reported a numerical study of steady state laminar forced and free convective and radiative heat transfer in an inclined rotating rectangular duct with a centered circular tube for a hydro dynamically

fully developed flow. The coupled equations of momentum and energy transports were solved using Gauss-Seidel iteration technique subjected to given boundary conditions. A thermal boundary condition of uniform wall temperature in the flow direction was considered. Results for mean and total mean Nusselt numbers for various values of Reynolds number (Re), Rayleigh number (Ra), Geometric ratio (GR), aspect ratio (AR), Radiation-Conduction parameter (N), Optical thickness ( $\hat{t}$ ), Rotational Reynolds number (Ro) and Emissivity ( $\epsilon$ ) were presented. For the range of parameters considered. The results indicated that heat transfer from the surface of the circle exceeds that of the rectangle. Optimum heat transfer and fluid bulk temperature were attained when the duct was vertically positioned.

Previous work studied the case of the fully developed laminar mixed convective heat transfer in an inclined concentric cylindrical annulus without the effect of radiation, the present work will be investigate the case with radiation.

**MATHEMATICAL MODEL:**

The effect of radiation and heat generation will be investigated for fully developed laminar mixed convective heat transfer in an inclined concentric cylindrical annulus shown in **Fig. 1**, for thermal boundary condition of constant heat flux on the inner cylinder and constant wall temperature at the outer cylinder.

Unsteady steady state, quasi three-dimensional, incompressible, fully developing laminar aiding air flow will be investigated. Accordingly the governing, continuity, momentum and

energy conservation equations are as follows:-

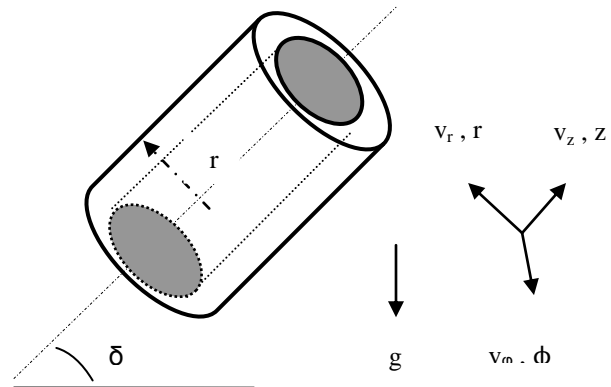


Fig. 1 Three Dimensional Annular Geometry

**Continuity equation:**

$$\frac{\partial u}{\partial x} + \frac{\partial v}{\partial y} = 0 \tag{1}$$

**Momentum Equations:**

$$\frac{\partial u}{\partial t} + u \frac{\partial u}{\partial x} + v \frac{\partial u}{\partial y} = -\frac{1}{\rho} \frac{dp}{dx} + \nu \left[ \frac{\partial^2 u}{\partial x^2} + \frac{\partial^2 u}{\partial y^2} \right] \tag{2}$$

$$\frac{\partial v}{\partial t} + u \frac{\partial v}{\partial x} + v \frac{\partial v}{\partial y} = -\frac{1}{\rho} \frac{dp}{dy} + \nu \left[ \frac{\partial^2 v}{\partial x^2} + \frac{\partial^2 v}{\partial y^2} \right] + g\beta(T - T_w) \tag{3}$$

$$\frac{\partial w}{\partial t} + u \frac{\partial w}{\partial x} + v \frac{\partial w}{\partial y} = -\frac{1}{\rho} \frac{dp}{dz} + \nu \left[ \frac{\partial^2 w}{\partial x^2} + \frac{\partial^2 w}{\partial y^2} \right] \tag{4}$$

**Energy Equation:**

$$\frac{\partial T}{\partial t} + u \frac{\partial T}{\partial x} + v \frac{\partial T}{\partial y} + w \frac{\partial T}{\partial z} = \alpha \left[ \frac{\partial^2 T}{\partial x^2} + \frac{\partial^2 T}{\partial y^2} \right] + \frac{4\sigma k_f \epsilon T_w^3}{\rho c_p} (T_w - T) \tag{5}$$

**The dimensionless parameters:**

$$\tau = \frac{\nu t}{De^2}, De = 2(r_o - r_i),$$

$$X = \frac{x}{De}, Y = \frac{y}{De}, \quad \frac{\partial \Omega}{\partial \tau} + U \frac{\partial \Omega}{\partial X} + V \frac{\partial \Omega}{\partial Y} = \left[ \frac{\partial^2 \Omega}{\partial X^2} + \frac{\partial^2 \Omega}{\partial Y^2} \right] - Ra \frac{\partial \theta}{\partial X}$$

$$Z = \frac{z}{De}, \quad \varepsilon = \frac{\varepsilon}{De}, \quad U = \frac{uDe}{\nu}, \quad V = \frac{vDe}{\nu}, \quad (11)$$

$$W = \frac{wDe}{\nu}, \quad \theta = \frac{(T_w - T)}{PrCDe}, \quad P = \frac{PDe^2}{\rho \nu^2},$$

$$Pr = \frac{\nu}{\alpha}, \quad Ra = \frac{g\beta CDe^4}{\nu\alpha}, \quad C = \frac{\partial T}{\partial z},$$

$$A = -\frac{4\rho\nu^2 Re}{De^3},$$

$$\hat{R} = \frac{r_o}{r_i}, \quad N = \frac{4\sigma\varepsilon T_w^3}{k k_r}, \quad \hat{t} = k_r De$$

By using these dimensionless forms, the above equations can be written as follows.

$$\frac{\partial U}{\partial X} + \frac{\partial V}{\partial Y} = 0 \quad (6)$$

$$\frac{\partial U}{\partial \tau} + U \frac{\partial U}{\partial X} + V \frac{\partial U}{\partial Y} = -\frac{dP}{dX} + \left[ \frac{\partial^2 U}{\partial X^2} + \frac{\partial^2 U}{\partial Y^2} \right] \quad (7)$$

$$\frac{\partial V}{\partial \tau} + U \frac{\partial V}{\partial X} + V \frac{\partial V}{\partial Y} = -\frac{dP}{dY} + \left[ \frac{\partial^2 V}{\partial X^2} + \frac{\partial^2 V}{\partial Y^2} \right] - Ra \theta \quad (8)$$

$$\frac{\partial W}{\partial \tau} + U \frac{\partial W}{\partial X} + V \frac{\partial W}{\partial Y} = \left[ \frac{\partial^2 W}{\partial X^2} + \frac{\partial^2 W}{\partial Y^2} \right] + 4Re \quad (9)$$

$$\frac{\partial \theta}{\partial \tau} + U \frac{\partial \theta}{\partial X} + V \frac{\partial \theta}{\partial Y} = \frac{1}{Pr} \left[ \frac{\partial^2 \theta}{\partial X^2} + \frac{\partial^2 \theta}{\partial Y^2} \right] + \frac{W}{Pr} + \frac{N\hat{t}^2\theta}{Pr} \quad (10)$$

The governing equations in dimensionless form above were written in terms of dependant variables ( $U, V, W, P, \theta$ ). The pressure term in the momentum equations will be eliminated in the resulting vorticity equation as can be shown:

For this flow field, the only non-zero component of the vorticity is:

$$\Omega = \frac{\partial V}{\partial X} - \frac{\partial U}{\partial Y} \quad (12)$$

Also by making use of the vorticity definition of Eq. 12 and the definition of stream function ( $\Psi$ ), which satisfy continuity equation, the horizontal and vertical velocities can be written as follows respectively:-

$$U = \frac{\partial \Psi}{\partial Y} \quad (13)$$

$$V = -\frac{\partial \Psi}{\partial X} \quad (14)$$

By substituting the velocity components of Eq. 13 and Eq. 14 in the vorticity definition equation (12), stream function equation resulted as:-

$$-\Omega = \left[ \frac{\partial^2 \Psi}{\partial X^2} + \frac{\partial^2 \Psi}{\partial Y^2} \right] \quad (15)$$

### Initial Conditions:

Initial conditions may be chosen as zero:

At  $\tau = 0$ ,  $U = V = W = \Omega = \Psi = 0$   
[No slip condition]

The boundary conditions which defined by **Kotake and Hattori [5]** and **Kaviany [6]** make use the boundary conditions for a motionless rigid surface which required that both horizontal and vertical velocities components (U and V) to be vanished at surface.

This expressed in terms of stream function as follows:-

- Inner cylinder surface :

$$U = V = W = \Psi = 0 \quad ,$$

$$\Omega = \frac{\partial^2 \Psi}{\partial Y^2} \Big|_w \quad , \quad \theta_i = 0$$

(16)

- Outer cylinder surface :

$$U = V = W = \Psi = 0 \quad ,$$

$$\Omega = - \frac{\partial^2 \Psi}{\partial Y^2} \Big|_w \quad , \quad \frac{\partial \theta_o}{\partial n} = 0$$

(17)

### TRANSFORMATION OF GOVERNING EQUATIONS:-

Governing equations can be transformed from the Cartesian coordinates (X, Y) to generalized coordinates ( $\zeta, \eta$ ) as shown below

#### Fletcher [7]:

- 1- Vorticity-Transport equation:-

$$\frac{\partial \Omega}{\partial \tau} + \frac{(\Psi_\eta \Omega_\zeta - \Psi_\zeta \Omega_\eta)}{J} = \frac{(\rho \Omega_\zeta + \omega \Omega_\eta + \alpha \Omega_{\zeta\zeta} - 2\beta \Omega_{\zeta\eta} + \gamma \Omega_{\eta\eta})}{J^2} - Ra \frac{(\theta_\zeta Y_\eta - \theta_\eta Y_\zeta)}{J}$$

(18)

- 2- Axial Momentum Equation:-

$$\frac{\partial W}{\partial \tau} + \frac{(\Psi_\eta W_\zeta - \Psi_\zeta W_\eta)}{J} = \frac{(\rho W_\zeta + \omega W_\eta + \alpha W_{\zeta\zeta} - 2\beta W_{\zeta\eta} + \gamma W_{\eta\eta})}{J^2} + 4Re$$

(19)

- 3- Energy equation:-

$$\frac{\partial \theta}{\partial \tau} + \frac{(\Psi_\eta \theta_\zeta - \Psi_\zeta \theta_\eta)}{J} = \frac{1}{Pr} \left[ \frac{(\rho \theta_\zeta + \omega \theta_\eta + \alpha \theta_{\zeta\zeta} - 2\beta \theta_{\zeta\eta} + \gamma \theta_{\eta\eta})}{J^2} + W + Nt^2 \theta \right]$$

(20)

- 4- Stream Function Equation:-

$$-\Omega = \frac{(\rho \Psi_\zeta + \omega \Psi_\eta + \alpha \Psi_{\zeta\zeta} - 2\beta \Psi_{\zeta\eta} + \gamma \Psi_{\eta\eta})}{J^2}$$

(21)

- 5- Vertical Velocity:-

$$V = \frac{(\Psi_\eta Y_\zeta - \Psi_\zeta Y_\eta)}{J}$$

(22)

- 6- Horizontal Velocity:-

$$U = \frac{(\Psi_\eta X_\zeta - \Psi_\zeta X_\eta)}{J}$$

(23)

### NUMERICAL SOLUTION:

Explicit finite difference technique was the numerical method used for solving the transient behavior of the fluid flow and heat transfer until the steady state was reached by marching out in time steps ( $\Delta\tau$ ) **Anderson [8]**.

#### Discretization of Vorticity

##### Equation:

$$\Omega_{(i,j)}^{n+1} = A_1 \Omega_{(i+1,j)}^n + A_2 \Omega_{(i-1,j)}^n + A_3 \Omega_{(i,j)}^n + A_4 \Omega_{(i,j+1)}^n + A_5 \Omega_{(i,j-1)}^n - A_6 (\Omega_{(i+1,j+1)}^n - \Omega_{(i+1,j-1)}^n - \Omega_{(i-1,j+1)}^n + \Omega_{(i-1,j-1)}^n) - A_7$$

(24)

Where:-

$$A_1 = \frac{\rho_{(i,j)} \Delta\tau}{2J_{(i,j)}^2 \Delta\zeta} + \frac{\alpha_{(i,j)} \Delta\tau}{J_{(i,j)}^2 \Delta\zeta^2} - \frac{E \Delta\tau}{4\Delta\zeta \Delta\eta J_{(i,j)}}$$

(25-a)

$$A_2 = - \frac{\rho_{(i,j)} \Delta\tau}{2J_{(i,j)}^2 \Delta\zeta} + \frac{\alpha_{(i,j)} \Delta\tau}{J_{(i,j)}^2 \Delta\zeta^2} + \frac{E \Delta\tau}{4\Delta\zeta \Delta\eta J_{(i,j)}}$$

(25-b)

$$A_3 = 1 - \frac{2\alpha_{(i,j)}\Delta\tau}{J_{(i,j)}^2\Delta\zeta^2} - \frac{2\gamma_{(i,j)}\Delta\tau}{J_{(i,j)}^2\Delta\eta^2} \quad (25-c)$$

$$A_4 = \frac{\varpi_{(i,j)}\Delta\tau}{2J_{(i,j)}^2\Delta\eta} + \frac{\gamma_{(i,j)}\Delta\tau}{J_{(i,j)}^2\Delta\eta^2} + \frac{F\Delta\tau}{4\Delta\zeta\Delta\eta J_{(i,j)}} \quad (25-d)$$

$$A_5 = -\frac{\varpi_{(i,j)}\Delta\tau}{2J_{(i,j)}^2\Delta\eta} + \frac{\gamma_{(i,j)}\Delta\tau}{J_{(i,j)}^2\Delta\eta^2} - \frac{F\Delta\tau}{4\Delta\zeta\Delta\eta J_{(i,j)}} \quad (25-e)$$

$$A_6 = \frac{\beta_{(i,j)}\Delta\tau}{2J_{(i,j)}^2\Delta\zeta\Delta\eta} \quad (25-f)$$

$$A_7 = \frac{Ra\Delta\tau}{J_{(i,j)}} \left[ \left( \frac{\theta_{(i+1,j)} - \theta_{(i,j)}}{2\Delta\zeta} * \frac{Y_{(i,j+1)} - Y_{(i,j-1)}}{2\Delta\eta} \right) - \left( \frac{\theta_{(i,j+1)} - \theta_{(i,j-1)}}{2\Delta\eta} * \frac{Y_{(i+1,j)} - Y_{(i-1,j)}}{2\Delta\zeta} \right) \right] \quad (25-g)$$

**Discretization of Axial Momentum Equation:**

$$W_{(i,j)}^{n+1} = B_1 W_{(i+1,j)}^n + B_2 W_{(i-1,j)}^n + B_3 W_{(i,j)}^n + B_4 W_{(i,j+1)}^n + B_5 W_{(i,j-1)}^n - B_6 (W_{(i+1,j+1)}^n - W_{(i+1,j-1)}^n - W_{(i-1,j+1)}^n + W_{(i-1,j-1)}^n) + B_7 \quad (26)$$

Where:-

$$B_1 = \frac{\varrho_{(i,j)}\Delta\tau}{2J_{(i,j)}^2\Delta\zeta} + \frac{\alpha_{(i,j)}\Delta\tau}{J_{(i,j)}^2\Delta\zeta^2} - \frac{E\Delta\tau}{4\Delta\zeta\Delta\eta J_{(i,j)}} \quad (27-a)$$

$$B_2 = -\frac{\varrho_{(i,j)}\Delta\tau}{2J_{(i,j)}^2\Delta\zeta} + \frac{\alpha_{(i,j)}\Delta\tau}{J_{(i,j)}^2\Delta\zeta^2} + \frac{E\Delta\tau}{4\Delta\zeta\Delta\eta J_{(i,j)}} \quad (27-b)$$

$$B_3 = 1 - \frac{2\alpha_{(i,j)}\Delta\tau}{J_{(i,j)}^2\Delta\zeta^2} - \frac{2\gamma_{(i,j)}\Delta\tau}{J_{(i,j)}^2\Delta\eta^2} \quad (27-c)$$

$$B_4 = \frac{\varpi_{(i,j)}\Delta\tau}{2J_{(i,j)}^2\Delta\eta} + \frac{\gamma_{(i,j)}\Delta\tau}{J_{(i,j)}^2\Delta\eta^2} + \frac{F\Delta\tau}{4\Delta\zeta\Delta\eta J_{(i,j)}} \quad (27-d)$$

$$B_5 = -\frac{\varpi_{(i,j)}\Delta\tau}{2J_{(i,j)}^2\Delta\eta} + \frac{\gamma_{(i,j)}\Delta\tau}{J_{(i,j)}^2\Delta\eta^2} - \frac{F\Delta\tau}{4\Delta\zeta\Delta\eta J_{(i,j)}} \quad (27-e)$$

$$B_6 = \frac{\beta_{(i,j)}\Delta\tau}{2J_{(i,j)}^2\Delta\zeta\Delta\eta} \quad (27-f)$$

$$B_7 = \Delta\tau(4Re - Ra\theta_{(i,j)} \sin \delta) \quad (27-g)$$

**Discretization of Energy Equation:**

$$\theta_{(i,j)}^{n+1} = C_1 \theta_{(i+1,j)}^n + C_2 \theta_{(i-1,j)}^n + C_3 \theta_{(i,j)}^n + C_4 \theta_{(i,j+1)}^n + C_5 \theta_{(i,j-1)}^n - C_6 (\theta_{(i+1,j+1)}^n - \theta_{(i+1,j-1)}^n - \theta_{(i-1,j+1)}^n + \theta_{(i-1,j-1)}^n) + C_7 \quad (28)$$

Where:-

$$C_1 = \frac{\varrho_{(i,j)}\Delta\tau}{2Pr J_{(i,j)}^2\Delta\zeta} + \frac{\alpha_{(i,j)}\Delta\tau}{Pr J_{(i,j)}^2\Delta\zeta^2} - \frac{E\Delta\tau}{4\Delta\zeta\Delta\eta J_{(i,j)}} \quad (29-a)$$

$$C_2 = -\frac{\varrho_{(i,j)}\Delta\tau}{2Pr J_{(i,j)}^2\Delta\zeta} + \frac{\alpha_{(i,j)}\Delta\tau}{Pr J_{(i,j)}^2\Delta\zeta^2} + \frac{E\Delta\tau}{4\Delta\zeta\Delta\eta J_{(i,j)}} \quad (29-b)$$

$$C_3 = 1 - \frac{2\alpha_{(i,j)}\Delta\tau}{Pr J_{(i,j)}^2\Delta\zeta^2} - \frac{2\gamma_{(i,j)}\Delta\tau}{Pr J_{(i,j)}^2\Delta\eta^2} \quad (29-c)$$

$$C_4 = \frac{\varpi_{(i,j)}\Delta\tau}{2Pr J_{(i,j)}^2\Delta\eta} + \frac{\gamma_{(i,j)}\Delta\tau}{Pr J_{(i,j)}^2\Delta\eta^2} + \frac{F\Delta\tau}{4\Delta\zeta\Delta\eta J_{(i,j)}} \quad (29-d)$$

$$C_5 = -\frac{\varpi_{(i,j)}\Delta\tau}{2Pr J_{(i,j)}^2\Delta\eta} + \frac{\gamma_{(i,j)}\Delta\tau}{Pr J_{(i,j)}^2\Delta\eta^2} - \frac{F\Delta\tau}{4\Delta\zeta\Delta\eta J_{(i,j)}} \quad (29-e)$$

$$C_6 = \frac{\beta_{(i,j)}\Delta\tau}{2Pr J_{(i,j)}^2\Delta\zeta\Delta\eta} \quad (29-f)$$

$$C_7 = \left[ \frac{(W_{(i,j)} + Q_{(i,j)} + Nt^2\theta_{(i,j)})}{Pr} \right] \Delta\tau \quad (29-g)$$

$$E = \Psi_{(i,j+1)} - \Psi_{(i,j-1)} \quad (29-h)$$

$$F = \Psi_{(i+1,j)} - \Psi_{(i-1,j)} \quad (29-i)$$

**Stream Function Solving Method:**

$$\Psi_{(i,j)}^{n+1} = \Psi_{(i,j)}^n + \sigma(\Psi_{(i,j)}^{n+1} - \Psi_{(i,j)}^n) \quad (30)$$

**Calculation of Average Axial Velocity:**

$$\bar{W} = (\sum_{i,j}^{Ni,Nj} W_{(i,j)} J_{(i,j)}) / J \quad (31)$$

**Calculation of Bulk Temperature:**

$$\theta_b = (\sum_{i,j}^{Ni,Nj} \theta_{(i,j)} W_{(i,j)} J_{(i,j)}) / \bar{W} J \quad (32)$$

**Calculation of Nusselt Number:**

$$Nu_b = \frac{W_{(i,j)}(\hat{R}+1)}{4\theta_{b(i,j)}} \quad (33)$$

**RESULTS AND DISCUSSION:**

**Streamlines And Isotherms:**

**Figs. 2a, b, c and d**, display the temperature distribution and the secondary flow pattern in the cross section of the annulus for Ra=200, Re=50, Pr=0.7 and  $\hat{R}=2.6$  with different values of inclination angle  $\delta$ .

The value of  $\Psi_{max}$  listed for each pattern which is a measure of the strength of the secondary flow;  $\Psi_{max}$  is the maximum value of the dimensionless stream function  $\Psi$ .

**1- Horizontal Position:**

**Fig. 2-a**, shows that for  $\delta=0^\circ$  (Horizontal) and low Rayleigh number (Ra=200), the secondary flow is weak ( $\Psi_{max}=1.9027$ ), and forms a symmetrical eddy rotating in the clockwise and anti-clockwise direction (i.e., there is one cell only in each side). Thus, the isotherms

are nearly circular and thus little affected by the secondary currents.

**2- Inclined Position:**

It is expected that the heat transfer process in horizontal position is better than other angles of inclination because of the stronger secondary flows associated with free convection which behave so as to reduce temperature difference in the annulus. In general, in horizontal and inclined positions, the fluid flows up along the inner wall to form vorticities having their center in the upper part of the annulus. **Figs. 2b and 2c**, show the effect of inclination angle on the heat and fluid flow patterns for Ra=200, Re=50, Pr=0.7,  $\hat{R}=2.6$  for angles of inclination ( $30^\circ$  and  $60^\circ$ ); respectively. It is clear from these figures that there is a slight effect on the streamlines behavior and more pronounced effect on isotherm lines. The isotherms tend to be more circular as angle of inclination deviates from horizontal to vertical position.

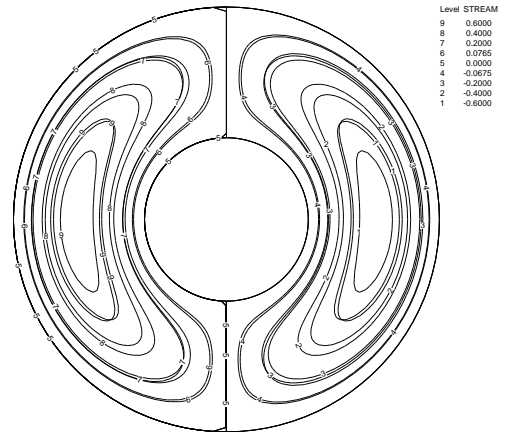
**3- Vertical Position:**

In vertical position, the velocities due to buoyancy forces are parallel to the direction of the forced motion; thus, rotational symmetry is retained. This situation leads to one component of the velocity due to buoyancy forces in the same direction of axial velocity because there are no components of buoyancy forces in (X, Y) direction compares with the horizontal and inclined positions in which three components of velocity in (X, Y, Z) directions are formed. Thus, there is no tangential velocity (V) and radial velocity (U), and the value of stream function in terms of these two velocities is equal to zero. Therefore, in vertical position the main and secondary flows are in the same direction, so the

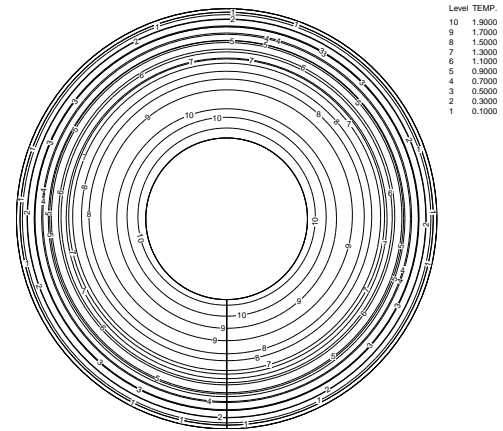
vortex strength diminishes. **Fig. 2d**, represent the effect of inclination angle on the isotherm lines contour for  $Ra=200$ ,  $Re=50$ ,  $Pr=0.7$  and  $\delta=90^\circ$  (vertical); as can be seen from these figures, it is impossible to represent the secondary flow by plotting a diagram describes streamlines since stream function is equal to zero. This is a guide for accuracy of the numerical method used in solution of the governing equations of flow.

The figures show that the isotherm lines seem to be close to each other near the heated inner wall because the natural convection is weak ( $Ra=200$ ) and have a slight effect on the flow field compared with forced convection . This effect is

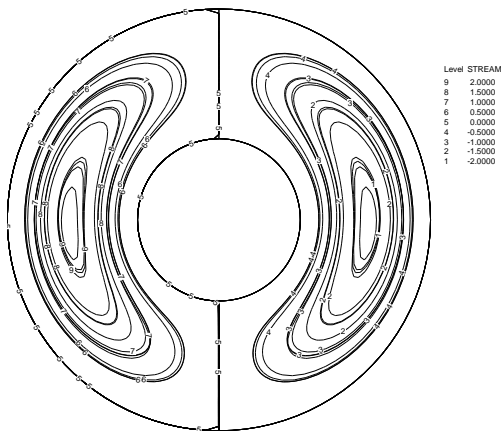
(a)  $\delta = 0^\circ$  Isotherms



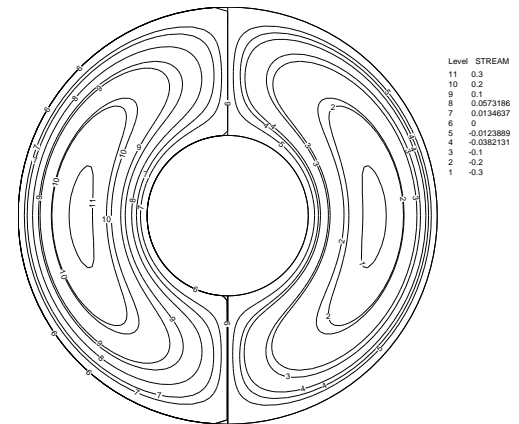
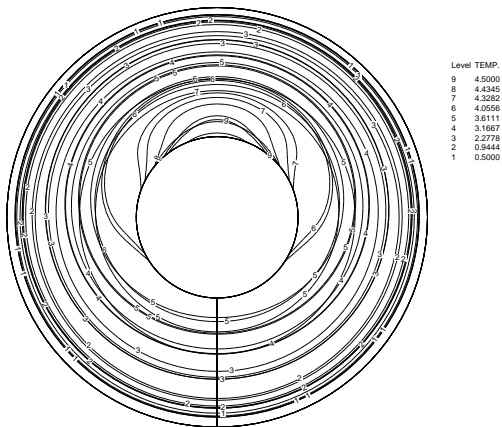
(a)  $\delta = 30^\circ$  Streamlines



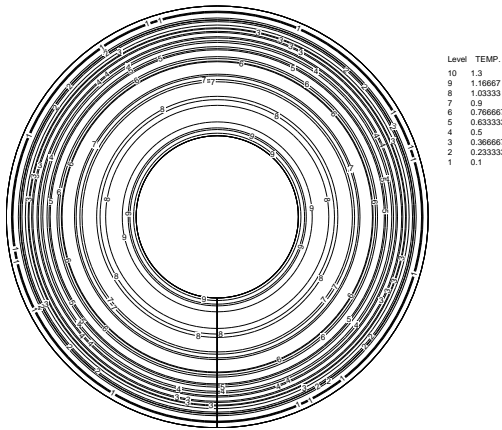
(b)  $\delta = 30^\circ$  Isotherms



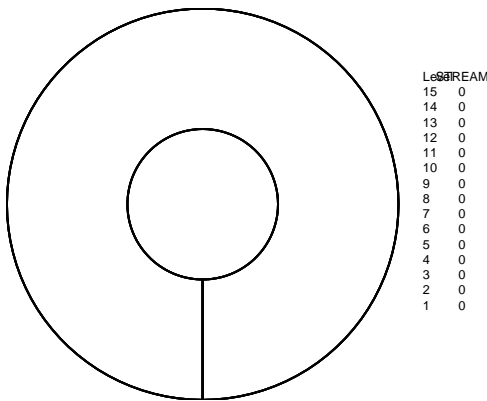
(a)  $\delta = 0^\circ$  Streamlines



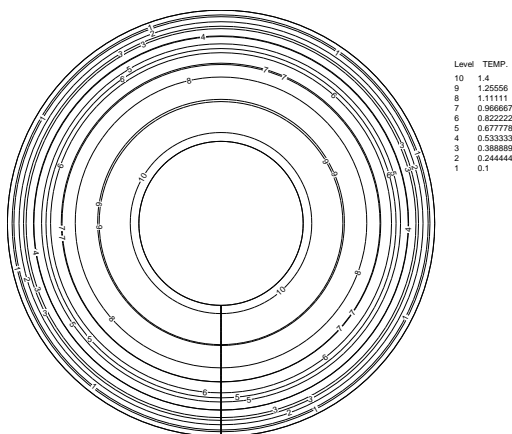
(c)  $\delta = 60^\circ$  Streamlines



(c)  $\delta = 60^\circ$  Isotherms



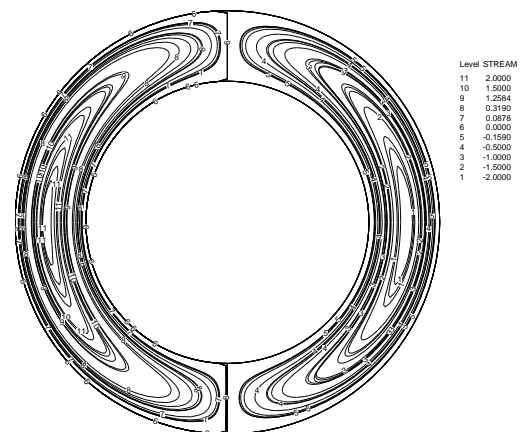
(d)  $\delta = 90^\circ$  Streamlines



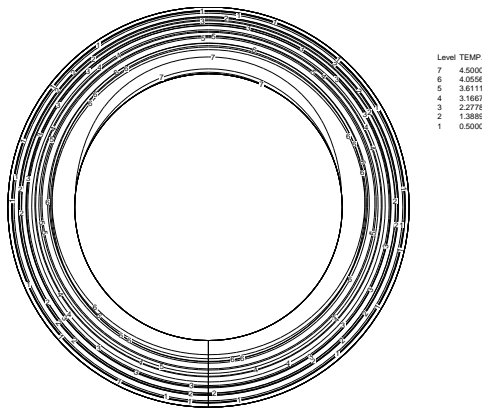
(d)  $\delta = 90^\circ$  Isotherms

Fig. 2a,b,c,d Streamlines and Isotherms for  $Ra=200, Re=50, Q=0, \hat{R}=2.6, N=3,$  and  $\hat{t}=1$  limited to accelerate the fluid velocity near the heated wall. Since this study was achieved in the region of thermally and hydraulic fully developed, then the isotherm lines remain in a form of circular lines which have the same center located at the center of the annulus and distributed between the temperature of the heated inner wall and the adiabatic outer wall.

Streamlines and isotherms are shown in **Fig. 3**, with different  $\hat{R}$  which indicate that the radius ratio does not alter the qualitative features of the isotherm and streamline patterns. The strength of the secondary flow is seen to decrease with the increase in the radius ratio. When  $\hat{R}$  is large, the heated surface of the inner cylinder, near which the boundary force is greatest forms a relatively small portion of the boundary of the calculation domain, thus reducing the driving force for the secondary motion.

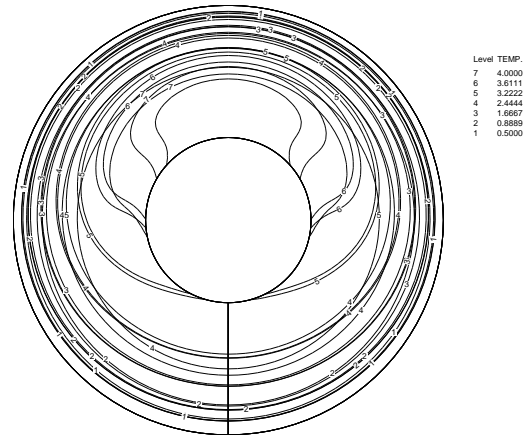


Streamlines



Isotherms

Fig. 3 Streamlines and Isotherms for  $Ra=200, Re=50, Q=0, \hat{R}=1.5, N=3,$  and  $\hat{\tau}=1$

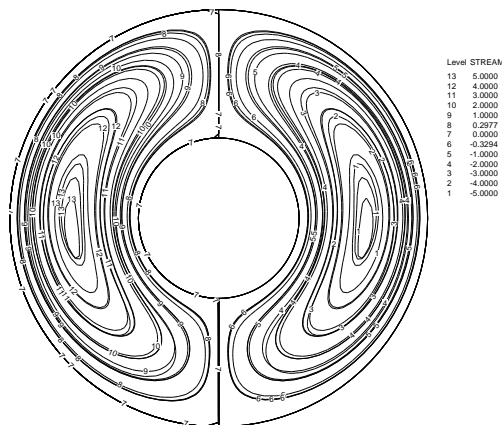


Isotherms

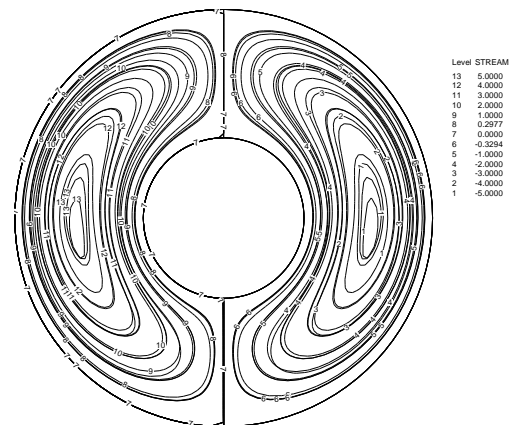
Fig. 4 Streamlines and Isotherms for  $Ra=600, Re=50, Q=0, \hat{R}=2.6, N=3,$  and  $\hat{\tau}=1$

For  $Ra=600$  in **Fig. 4**, the secondary flow was still weak ( $\Psi_{max}=4.7055$ ) and forms a symmetrical eddy rotating in the clockwise and anti-clockwise direction (i.e., there is one eddy only in each side).

**Fig. 5**, shows that the increase in  $Re$  will change the behavior of the stream function and the temperature distribution. Both stream function and temperature distribution of the air will be increase as  $Re$  increase, because as  $Re$  increase it will strengthen the vortex of the secondary flow. The flow pattern at  $Re=2000$  is similar to that at  $Re=1000$ .



Streamlines



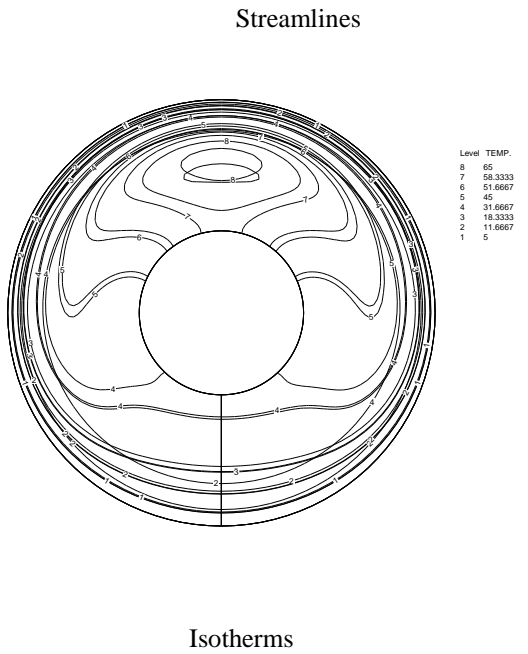


Fig. 5 Streamlines and Isotherms for  $Ra=200, Re=1000, Q=0, \hat{R}=2.6, N=3,$  and  $\hat{\tau}=1$

It is clear from **Fig. 6**, that there is a slight effect on the streamlines behavior and more pronounced effect on isotherm lines when  $Q$  increase and heat transfer increase as  $Q$  increase and this is due to the increase of the total heat gain by the air which leads to accelerate the flow of air.

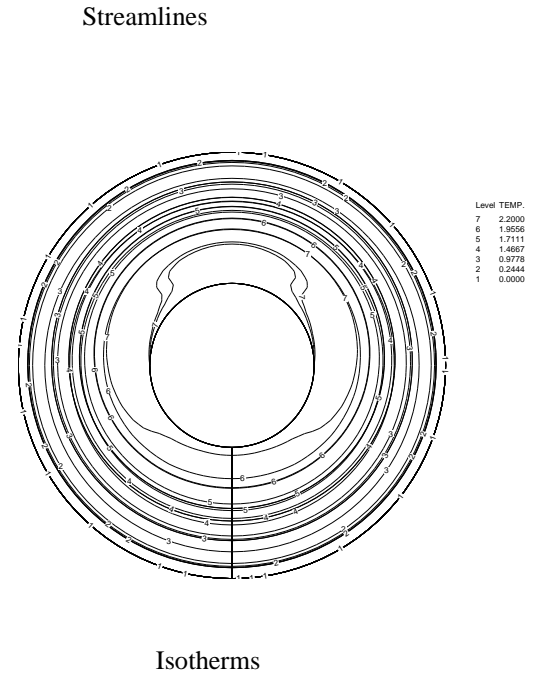


Fig. 6 Streamlines and Isotherms for  $Ra=200, Re=50, Q=10, \hat{R}=2.6, N=3,$  and  $\hat{\tau}=1$

**Fig. 7**, illustrates the effect of  $\delta$  on  $Nu$ . Generally,  $Nu$  will be increased with the increasing in the inclination angle  $\delta$ . This is because of the increasing in the effect of the buoyancy force component toward the flow direction which will accelerate the flow and heat transfer process and that result to increase the rate of heat transfer between the air and the walls of the annulus. Also, the effect of radiation is so clear and it increases

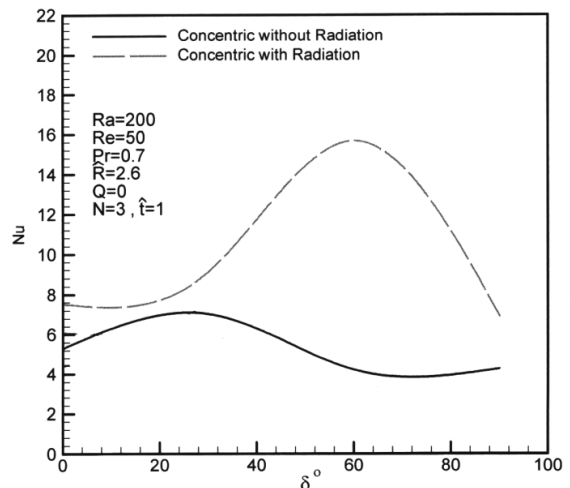
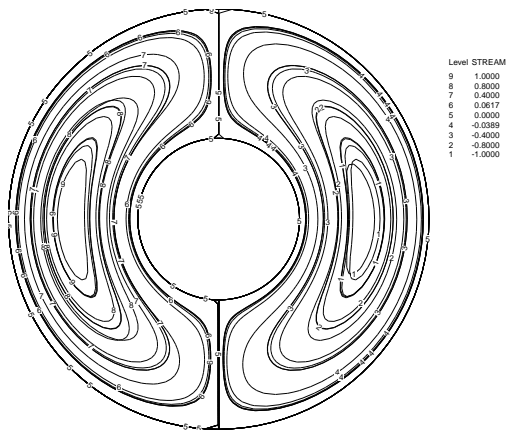


Fig. 7 Effect of inclination angle on Nu

the rate of heat transfer because of the heat gain that transformed to the air by radiation, therefore, the flow and the velocities of the air will be accelerated leading to increase in the rate of heat transfer.

**Effect Of Radius Ratio ( $\hat{R}$ ):**

**Fig. 8** illustrates the effect of radius ratio on Nu. The influence of buoyancy is to increase Nu but this becomes noticeable only after a threshold value of Ra exceeded. Thus as  $\hat{R}$  increased Nu increased, because heat is removed most

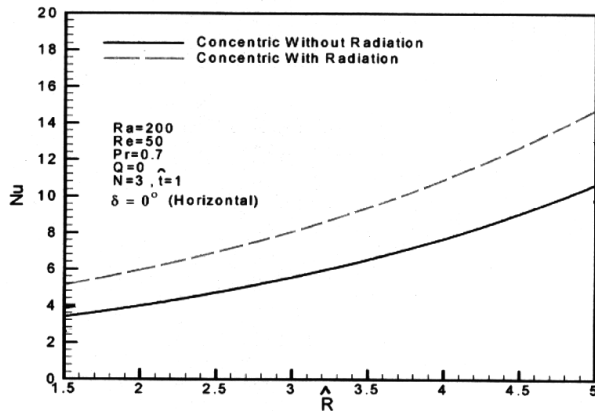


Fig. 8 Variation of Nu with  $\hat{R}$

efficiently from the inner heated wall for large value of  $\hat{R}$  and because for large  $\hat{R}$  the gap in the annulus would be relatively very large and even if heat is flowing into the fluid at a high rate it would be carried off downstream before it was able to penetrate very far across the gap. Therefore, as radius ratio grows, contribution of the convection to the overall heat transfer was increased contrary to the role of conduction.

The effect of inclination angle on the variation of Nu with  $\hat{R}$  is shown in **Fig. 9**. The figure shows that as  $\delta$  increased

Nu will be increased, this is because as  $\delta$  increased the effect of buoyancy force component toward the flow direction will accelerate the flow and heat transfer process.

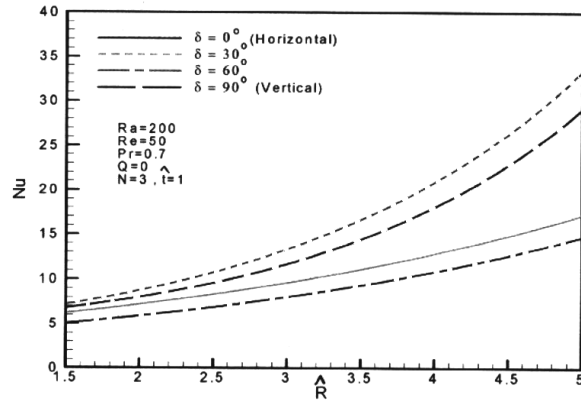


Fig. 9 Variation of Nu with  $\hat{R}$  for different values of  $\delta$

**Fig. 10**, illustrates the effect of Ra on Nu value with the variation of  $\hat{R}$ . The figure shows that the value of Nu increases as  $\hat{R}$  increases for each value of Ra, this is because as the radius ratio grows, contribution of the convection to the overall heat transfer increased contrary to the role of conduction.

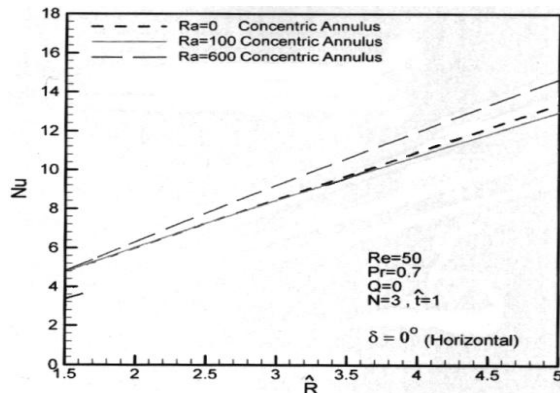


Fig. 10 Variation of Nu with  $\hat{R}$  for different values of Ra (horizontal annulus)

**Fig. 11**, illustrates the effect of Ra on Nu value with the variation of  $\hat{R}$  for vertical annulus. The figure shows relatively the same effect with that obtained in **Fig. 10**, which shows that the inclination angle has a little effect on the variation of  $\hat{R}$ .

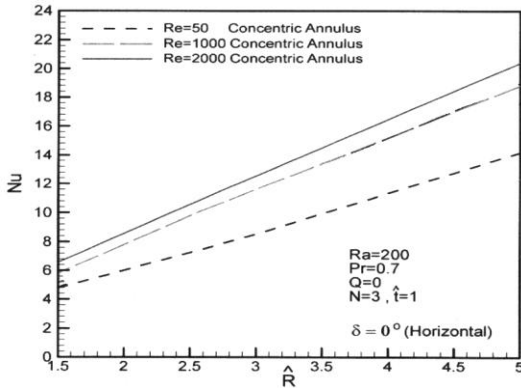


Fig. 11 Variation of Nu with  $\hat{R}$  for different values of Ra (vertical annulus)

In **Fig. 12**, it is clear that Nu will be increased as  $\hat{R}$  increased for each value of Re. This is due to the increase in the rate of heat transfer is because of the increase in Re and therefore, increase fluid flow.

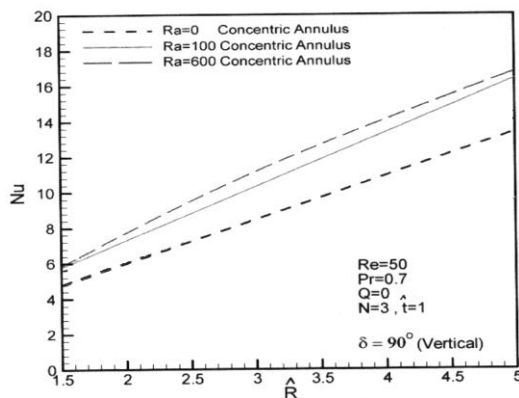


Fig. 12 Variation of Nu with  $\hat{R}$  for different values of Re (horizontal annulus)

**Fig. 13**, shows the effect of Re on Nu with the variation in  $\hat{R}$  for vertical annulus. In this figure for Re=50, 1000,

2000, Nu will be increased rapidly with the increase in  $\hat{R}$  and the curves for these two values of Re have the same shape and same value.

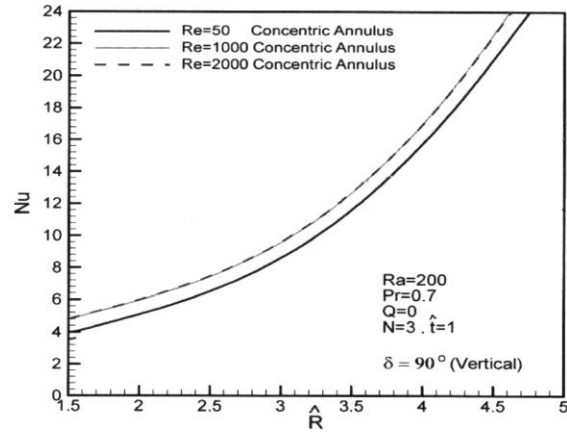


Fig. 13 Variation of Nu with  $\hat{R}$  for different values of Re vertical annulus

**Effect of Rayleigh Number (Ra):**

**Fig. 14**, shows that Nu will be increased as Ra increased because the vortex strength increases with Rayleigh number and this will increase the buoyancy effect resulting in an increase in the rate of heat transfer.

The radiation effect increases with the increasing in Ra because of the heat gain that transformed to the air by radiation. Therefore, the flow and the velocities of the air will be accelerated leading to increase in the rate of heat transfer.

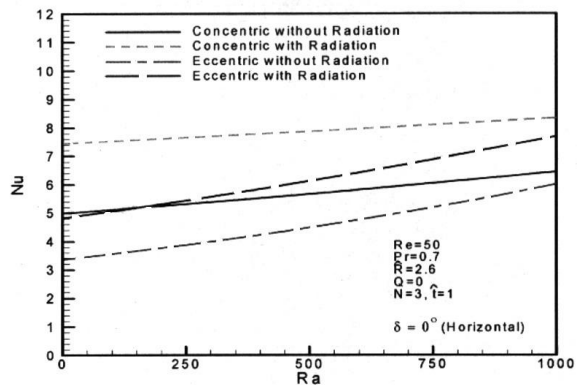


Fig. 14 Effect of Ra on Nu

**Fig. 15** shows that there is an optimum value of annulus inclination that gives maximum value of Nu, for most instance this max. which appears at  $90^\circ$  of annulus inclination.

Rayleigh number at which back flow occurs is of considerable theoretical and practical interest and the numerical results was given below for  $Pr=0.7$  and  $ReRa < 50,000$ . Because of the assumptions, the reversal flow cannot occur for the limiting case of horizontal annulus ( $\delta=0^\circ$ ) for the present problem.

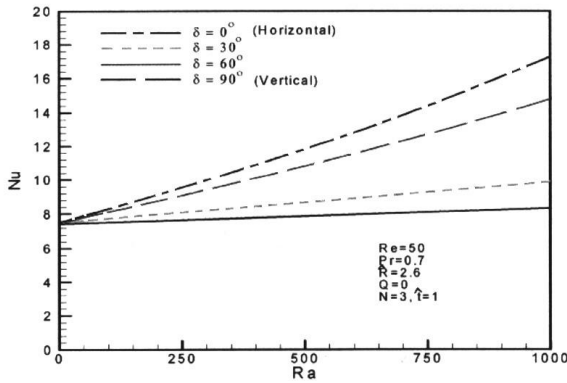


Fig. 15 Variation of Nu with Ra for different values of  $\delta$

**Effect Of Reynolds Number(Re):**

**Fig. 16**, shows that Nu will be increase in respect to the limiting condition of pure forced condition ( $Ra=0$ ). Until Re is less than the standard critical value of about 2000 and  $ReRa$  is far from the critical value ( $ReRa \leq 50000$ ) causing flow reversal conditions, heat transfer by mixed convection develops in stable laminar regime.

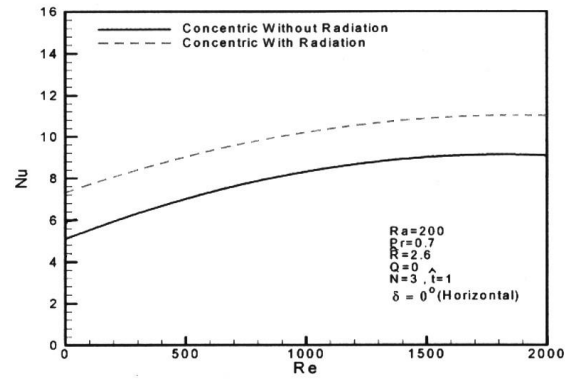


Fig. 16 Effect of Re on Nu

**Fig. 17**, shows that as  $\delta$  increase Nu will be increase and the higher value of Nu for low Re occurs at  $\delta=30^\circ$ , while the higher value of Nu for high Re occurs at  $\delta=0^\circ$ .

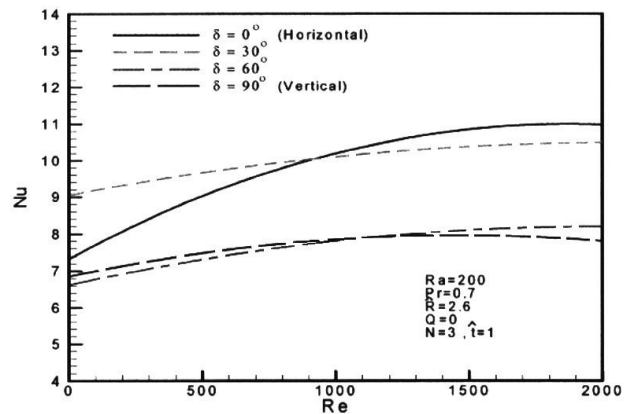


Fig. 17 Variation of Nu with Re for different values of  $\delta$

An improvement in Nu value is shown in **Fig. 18**, as Re increases for each Ra value. In fact, the highest Ra shows the highest Nu value. This behavior indicates that the secondary flow vorticities effect is high in high Re, but this effect will be diminishes for low Ra.

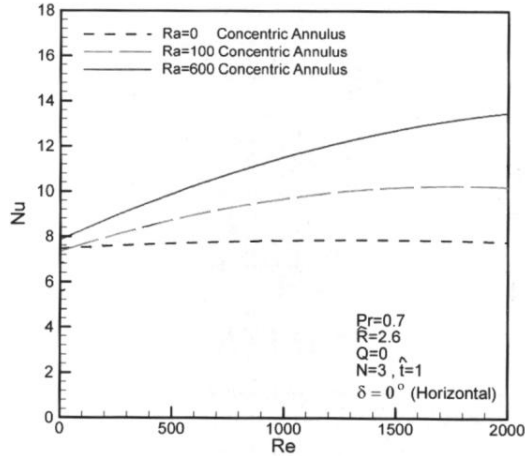


Fig. 18 Variation of Nu with Re for different values of Ra (horizontal annulus)

For a vertical annulus, **Fig. 19**, illustrates the effect of Ra on Nu with the variation in Re. Also, the figure shows an improvement in Nu value as Re increases for each Ra value. The increased value of Nu for vertical annulus was much higher than that for horizontal annulus because in the vertical case the direction of the buoyancy force components will be toward the flow direction and this will

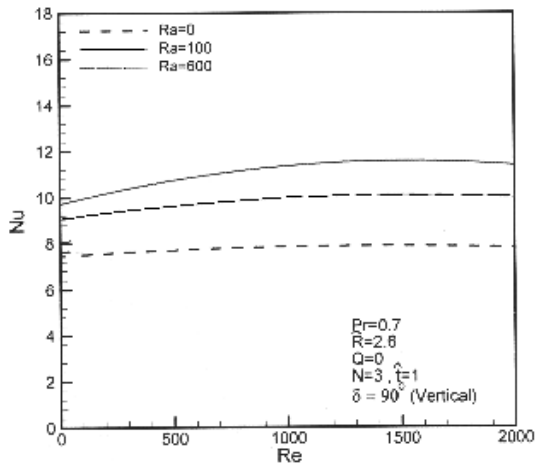


Fig.19 Variation of Nu with Re for different values of Ra (vertical annulus)

increase the rate of heat transfer. It is noticed from the figure that there is no

effect of inclination angle on Ra=0, i.e., for  $\delta=0^\circ, 90^\circ$  Ra has the same effect on Nu.

**Effect Of Radiation Properties:**

**Fig. 20**, shows that as conduction – radiation parameter N and optical thickness  $\hat{t}$  increase Nu will be increase, but the increase in  $\hat{t}$  will be greater than the increase in N, this is because the optical thickness is powered to 2 in the radiation term, so the radiation source term in the energy equation plays a more significant role, and the effect of radiation is augmented physically. For a higher N the participating medium contained between the two cylinders can be absorb more radiant energy and transform it in to thermal energy, thereby increasing the overall medium

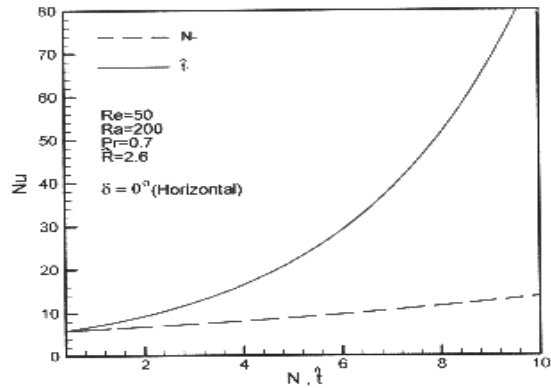


Fig. 20 Effect of radiation properties temperature compared with the non radiative case.

**COMPARISON OF RESULTS:**

Comparison is made for the value of Nu with different Ra for a vertical annulus with the results obtained by **Rogers and Yao [9]**. This comparison is shown in **Fig. 21**, from the foregoing figure a different (approximately 14%) is found between these results.

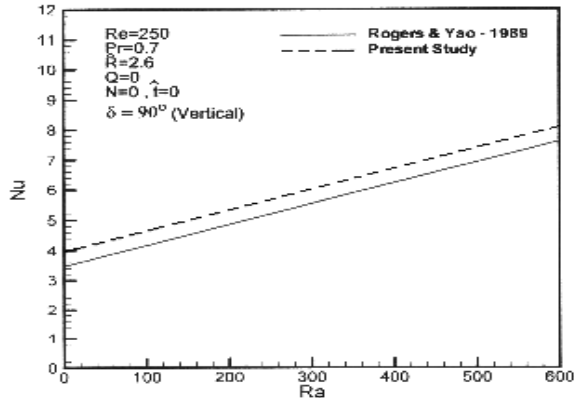


Fig. 21 Comparison of the present study with [9]

A correlation has been set up to give the average Nusselt number variation with Ra, M and N and Q. This correlation is made by using the computer program (DGA v1.00).

$$Nu = a_1 + a_2 Ra^{b_1} Re^{b_2} \bar{R}^{b_3} Q^{b_4} (\sin \delta)^{b_5} \tag{36}$$

Where, the constants in the correlation are defined in **Table 1**.

**Table 1 Constants in eq. 36**

Constants	Without radiation	With radiation
a <sub>1</sub>	5.35	7.54
a <sub>2</sub>	1.7	4.55
b <sub>1</sub>	9.13x10 <sup>-2</sup>	3.74x10 <sup>-2</sup>
b <sub>2</sub>	0.146	9.75x10 <sup>-2</sup>
b <sub>3</sub>	0.996	0.902
b <sub>4</sub>	3.77x10 <sup>-2</sup>	4.16x10 <sup>-2</sup>
b <sub>5</sub>	5.61x10 <sup>-2</sup>	5.84x10 <sup>-2</sup>

**CONCLUSIONS**

In the present work, a numerical investigation has been performed to examine the effect of radiation, inclination angle and the position of the inner cylinder of an annulus, on the rate of heat transfer for a fully developed, unsteady state laminar air flow .

The main results are as follows:

- 1- Nu increases with the increase in the inclination angle compared to the horizontal case. The maximum value of Nu seems to lie between (50°-70°).
- 2- Increasing the radius ratio of the annulus decreasing the resistance to the circulation motion which leads to faster replacement of the hot air adjacent to the inner cylinder by the cold air adjacent to the outer cylinder and this result in an increase in the rate of heat transfer.
- 3- Nu increased with the increase in Ra and Re, the secondary flow induced by buoyancy leads to a significant enhancement in heat transfer over the forced convection results.
- 4- Nu increases with the increase in the dimensionless heat generation Q from 0 to 10.
- 5- Radiation is found to play an important role in determining thermo fluid dynamics behavior in mixed convection in an annulus, when the radiation parameters (N, t) increase the radiation effect will also increase and this will increase the overall heat transfer.

**REFERENCES**

[1] Cheng K. C. and Hong S. W., (1972), "Combined Free and Forced Laminar Convection in Inclined Tubes", Appl. Sci. Res. 27, PP. 19-38.

[2] Bohne D. and Obermeier E., (1986), "Combined Free and Forced Convection in a Vertical and Inclined Cylindrical Annulus", Proceeding of the 8<sup>th</sup> Heat Transfer Conference, München, Fed. Ref. of Germany, Vol. 3, PP. 1401-1406.

[3] Akeel A. M. Al-Sudani, (2005), "An Investigation Into Laminar Combined Convection Heat Transfer Through Concentric Annuli", PhD. Thesis, University of Technology, Mechanical Engineering Department.

[4] Adegun I. K. and Bello-Ochevole F. L., (2004), "Mixed Convective and Radiative Heat Transfer in an Inclined Rotating Rectangular Duct With a Centered Circular Tube", J. of the Braz. Soc. Of Mech. Sci. & Eng., No. 3, Vol. XXVI, PP. 323-329.

[5] Kotake S. and Hattori N., (1985), "Combined Forced and Free Convection Heat Transfer for Fully –Developed Laminar Flow in Horizontal Annuli", J. Heat and Mass Transfer, No.11, Vol.28, PP. 2113-2120.

[6] Kaviany M., (1986), " Laminar Combined Convection in a Horizontal Annulus Subjected to Constant Heat Flux Inner Wall and Adiabatic Outer Wall", J. Heat Transfer, ASME, Vol. 108, PP. 392-397.

[7] Fletcher C. A. J., (1988), "Computational Fluid Techniques for Fluid Dynamics 2", Springer-Verlag.

[8] Anderson A. Tannehill C. and Pletcher H.,(1984), "Computational Fluid Mechanics and Heat Transfer", MC Graw-Hill, Washington.

[9] Rogers B. B. and Yao L. S., (1990), "The Effect of Mixed Convection Instability on Heat Transfer in a Vertical Annulus", Int. J. Heat and Mass Transfer, , No.1, Vol. 33, PP.79-90 .

**NOMENCLATURE**

**Latin Symbols:**

Symbol	Description	Unit
$\hat{R}$	Radius Ratio ( $\hat{R} = \frac{r_o}{r_i}$ )	---
$\hat{t}$	Optical Thickness ( $\hat{t} = k_r D_e$ )	---
A	Axial Pressure Gradient ( $A = -\frac{4\rho v^2 Re}{De^3}$ )	N/m <sup>3</sup>
C	Axial Temperature Gradient ( $C = \frac{\partial T}{\partial z}$ )	K/m
De	Hydraulic Diameter De = 2(r <sub>o</sub> - r <sub>i</sub> )	m
e	Space Between the Centers of the Inner and Outer Cylinders	m
g	Gravitational Acceleration	m/s <sup>2</sup>
J	Jacobean of Direct Transformation	---
k	Thermal Conductivity of the Air	W/m K
K <sub>r</sub>	Volumetric Absorption	m <sup>-1</sup>

	Coefficient	
N	Radiation-Conduction Parameter ( $N = \frac{4\sigma\epsilon T_w^3}{kk_r}$ )	---
n	Dimensionless Outer Normal Direction	---
Ni	Number of Gridlines in the $\phi$ -direction	---
Nj	Number of Gridlines in the r-direction	---
Nub	Bulk Nusselt Number	---
P	Normalized Air Pressure	---
p	Air Pressure	N/m <sup>2</sup>
Pr	Prandtl No. ( $Pr = \frac{\nu}{\alpha}$ )	---
Ra	Rayleigh Number ( $Ra = \frac{g\beta CDe^4}{\nu\alpha}$ )	---
Re	Reynolds Number ( $Re = \frac{ADe^3}{4\rho\nu^2}$ )	---
R <sub>i</sub>	Dimensionless Inner Cylinder Radius	---
r <sub>i</sub>	Inner Cylinder Radius	m
R <sub>o</sub>	Dimensionless Outer Cylinder Radius	---
r <sub>o</sub>	Outer Cylinder Radius	m
T	Air Temperature	K
t	Time	s

u, v, w	Velocity Components in x, y and z Direction Respectively	m/s
U, V, W	Dimensionless Velocity Components in X, Y and Z Direction Respectively	---
x, y, z	The physical Coordinates of The Annulus	m
X, Y, Z	The Dimensionless Physical Coordinates of The Annulus	---

### Greek Symbols

Symbol	Description	Unit
$\varrho, \overline{\omega}, \gamma$	Coefficient of Transformation of BFC.	---
$\phi_0$	Angular position for the inner cylinder	Degree
$\alpha$	Thermal Diffusivity	m <sup>2</sup> /s
$\beta$	Coefficient of Thermal Expansion	1/K
$\zeta, \eta$	Coordinates in the Transformed Domain	m
$\theta$	Dimensionless Air Temperature $\theta = \frac{(T_w - T)}{PrCDe}$	---
$\sigma$	Stefan Boltzmann	W/m <sup>2</sup> K <sup>4</sup>

	Constant	
$\tau$	Dimensionless Time $\tau = \frac{vt}{De^2}$	---
$\nu$	Kinematics' Air Viscosity	m/s <sup>2</sup>
$\Psi$	Dimensionless Air Stream Function	---
$\Omega$	Dimensionless Air Vorticity	---
$\epsilon$	Emissivity	---

### الخلاصة

تمت الدراسة العددية لأنتقال الطاقة الحرارية بالحمل المختلط-المشع لجريان غير مستقر خلال مجرى حلقي مائل . تم التعامل بميكانيكية إنتقال الطاقة الحرارية بالحمل والإشعاع بشكل منفصل وبالتعاقب. سطح الأسطوانة الخارجية بدرجة حرارة ثابتة والأسطوانة الداخلية سخنت بفيض حراري ثابت. الدراسة تضمنت الحل العددي للمعادلات الحاكمة (الإستمرارية، الزخم ومعادلة الطاقة) بإستخدام طريقة الفروق المحددة لإجراء جميع الحسابات باستخدام نظام مطابقة الإحداثيات لبناء شبكة النظام. تم بناء برنامج فورتران ٩٠ لحساب معدل رقم نسلت ( $Nu_b$ ) بعد الوصول إلى الحالة المستقرة لرقم براندتل ثابت (للهواء) ( $Pr = 0.7$ ) ولنسبة أقطار ( $R = 1.5, 2.6, 5.0$ ) ورقم رايلي ( $0 \leq Ra \leq 10^3$ ) ورقم رينولد ( $50 \leq Re \leq 2000$ ) وتولد حراري لابعدي ( $0 \leq Q \leq 10$ ) وبارامتر التوصيل- الإشعاع ( $0 \leq N \leq 10$ ) والسمك البصري ( $0 \leq t \leq 10$ ) ولزوايا ميل مختلفة مع المستوى الأفقي للمحتوى الحلقي لأسطوانتين متمركزتين. للمديات السابقة. النتائج بينت زيادة الطاقة الحرارية بتأثير الإشعاع وأن رقم نسلت  $Nu$  يزداد بزيادة زاوية الميل  $\delta$  و  $Q$ ,  $Ra$ ,  $Re$ , و  $\bar{R}$ . تم التوصل الى معادلات لمعرفة تأثير الإشعاع على عملية انتقال الحرارة. المقارنة مع البحوث السابقة أعطت نتائج متوافقة.